
**Liquid Crystals**
Publication details, including instructions for authors and subscription information:
http://www.informaworld.com/smpp/title~content=t713926090

# Chiral dopant induced twist grain boundary phases

I. Dierking[a]
[a] Institut für Physikalische Chemie, Technische Universität Darmstadt, Petersenstr. 20, D-64287 Darmstadt, Germany,

Online publication date: 06 August 2010

**To cite this Article** Dierking, I.(2001) 'Chiral dopant induced twist grain boundary phases', Liquid Crystals, 28: 2, 165 — 170
**To link to this Article: DOI:** 10.1080/02678290010005208
**URL:** http://dx.doi.org/10.1080/02678290010005208

LIQUID CRYSTALS, 2001, VOL. 28, NO. 2, 165–170

# Chiral dopant induced twist grain boundary phases

I. DIERKING*

Institut für Physikalische Chemie, Technische Universität Darmstadt,
Petersenstr. 20, D-64287 Darmstadt, Germany

(*Received 11 April 2000; in final form 22 May 2000; accepted 9 June 2000*)

A diarylethane α-chloro ester was mixed with a chiral dopant of high helical twisting power at variable concentration to study its capability for induction of twist grain boundary phases. With increasing concentration of the chiral dopant, TGBA* and TGBC* phases were observed with a rather broad region of existence. In contrast to homeotropic alignment, planar boundary conditions seem to enhance the phase stability of the TGB phases, resulting in metastable TGB states and phase coexistence with the respective smectic phases. The phase growth of SmA*/SmC* out of the TGBA*/TGBC* state was studied under isothermal conditions as a function of temperature and concentration of the chiral dopant.



## 1. Introduction

Twist grain boundary (TGB) phases are frustrated smectics resulting from a competition between chirality, i.e. the formation of helical superstructures, and thermodynamics, i.e. the formation of smectic layers. The two structural elements are not compatible with each other and defects have to be introduced. In the case of liquid crystalline TGBA*/TGBC* phases these defects are regular arrays of screw dislocations, forming grain boundaries between blocks with a local SmA*/SmC* symmetry [1]. Following the first experimental observation of a TGBA* phase by Goodby *et al.* [2], numerous reports on other compounds followed [3]. TGB phases can also be observed in mixtures of liquid crystal materials [4–8], as well as in liquid crystals doped with chiral materials [9]. In contrast to the usually rather narrow temperature region of TGB existence in single component systems, mixtures may exhibit broad ranges of TGB phases. Generally, TGB phases are observed only in highly chiral systems, i.e. materials with a short cholesteric pitch in the range of a few hundred nanometers.

Twist grain boundary phases exhibit three distinct structural features: (i) a helical superstructure, (ii) smectic layers and (iii) a helical axis parallel to the smectic layer plane. Despite the fact that TGBA* phases are smectic, their appearance in polarizing microscopic observation shows strong similarities to the cholesteric phase, which is generally the high temperature phase. Preparation under planar boundary conditions (director parallel to the substrate) often results in a Grandjean texture, while homeotropic alignment (director perpendicular to the substrate) generally shows the typical TGB filaments [10].

* Author for correspondence.
e-mail: dierking@hrzZ.hrz.tu-darmstadt.de

## 2. Experimental

A (chiral) diarylethane α-chloro ester compound, D8:

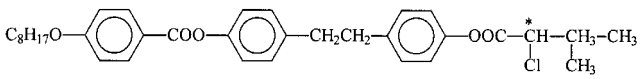

was chosen as the host material. This had been reported [11] to exhibit a very narrow TGBA* phase mediating the cholesteric and the SmA* phases. Its phase sequence on cooling is given by I 134 N* 129.4 TGBA* 129.2 SmA* 125.6 SmC* (°C) and higher ordered phases. A chiral dopant, here abbreviated as C4:

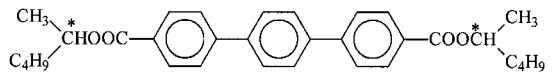

was added at different percentages by weight. Both materials were readily miscible even at large dopant concentrations. Texture studies were carried out using a polarizing microscope (Leitz) equipped with a Mettler hot stage and temperature controller giving an accuracy of relative temperatures within 0.1 K. Absolute temperatures are estimated to be accurate within 1 K. For the investigations, commercially available sandwich cells from E.H.C., Japan, were used with planar boundary conditions and a cell gap of 6 μm and with homeotropic boundary conditions with a gap of 10 μm. The growth dynamics of SmA* domains from the TGBA* phase were evaluated by video recording and subsequent image analysis by standard software (Adobe Premiere, Adobe Photoshop).

*Liquid Crystals* ISSN 0267-8292 print/ISSN 1366-5855 online © 2001 Taylor & Francis Ltd
http://www.tandf.co.uk/journals
DOI: 10.1080/02678290010005208

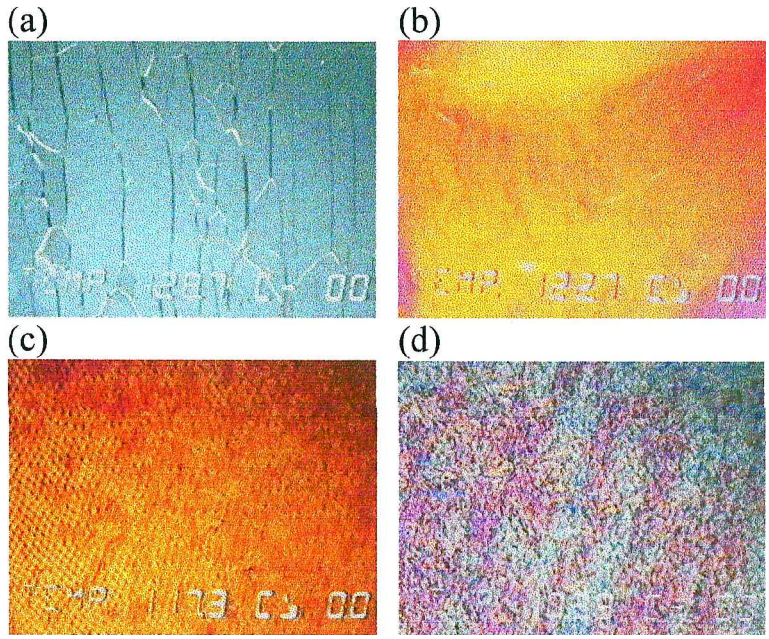


Figure 1. Texture photographs of the 95%D8 + 5%C4 mixture for planar boundary conditions. (*a*) Cholesteric Grandjean texture with oily-streaks. (*b*) Grandjean-like texture of the TGBA* phase, (*c*) two-dimensional periodicity of the square grid texture of TGBC*, and (*d*) SmC* phase. The image size is 290 µm × 220 µm.



## 3. Results and discussion

Typical textures obtained for mixtures (in wt %) of D8 and the chiral dopant C4 are illustrated for the 95%D8 + 5%C4 system, but are equivalent for all the other concentrations studied up to 20%C4. Figure 1 shows a sequence of textures obtained on cooling a sample with planar boundary conditions. The typical cholesteric Grandjean texture with oily-streaks is formed from the isotropic melt (*a*), before further cooling results in the transition into the TGBA* phase with a Grandjean-like texture (*b*), and then presumably a TGBC* phase with a characteristic two-dimensional periodicity of the

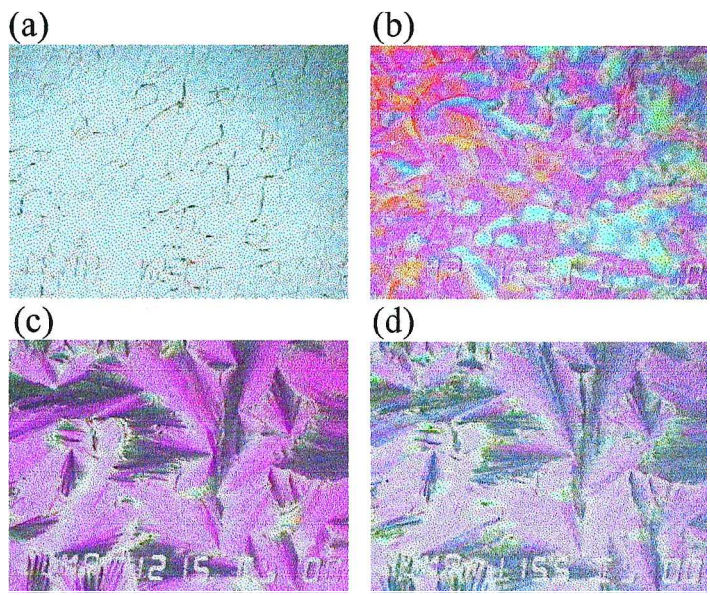


Figure 3. Texture photographs of the 95%D8 + 5%C4 mixture for homeotropic boundary conditions. In this preparation samples do not exhibit the expected textures for these boundary conditions, but rather give 'natural textures' as generally observed for untreated substrates. (*a*) Cholesteric phase, (*b*) TGBA* phase, (*c*) fan texture of SmA*, and (*d*) broken fan texture of SmC*. The image size is 290 µm × 220 µm.

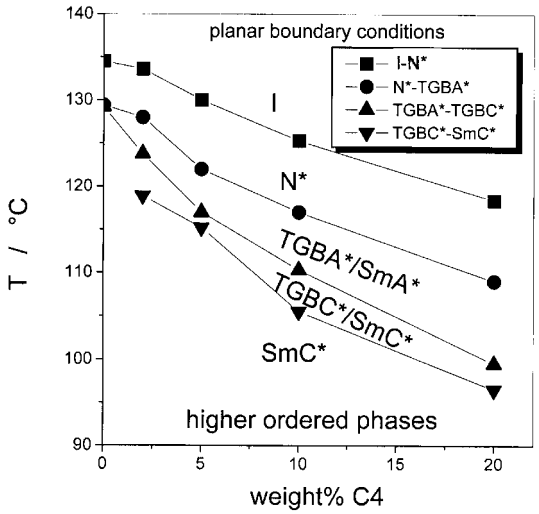


Figure 2. Phase diagram of the D8/C4 mixtures obtained by polarizing microscopic observation on samples prepared with planar boundary conditions.

square grid pattern [12, 13] (*c*), until at lower temperatures the SmC* phase (*d*) is formed. As the textural appearance of the three-dimensionally modulated UTGBC* phase reported in [14] is very similar, it can at this point not be stated conclusively which TGBC* structure is actually present. However, the general phase sequence I–N*–TGBA*–TGBC*–SmC*–higher ordered phases, can be concluded. Here, it has to be pointed out that in contrast to pure D8, the D8/C4 mixtures exhibit TGBA*/TGBC* textures, which are metastable in a certain temperature range. When kept under isothermal conditions, SmA*/SmC* regions nucleate and grow, a process which will be discussed in more detail below. Figure 2 summarizes the phase diagram of the D8/C4

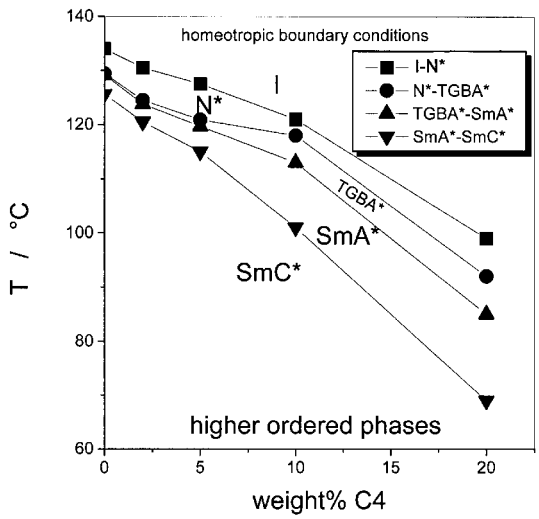


Figure 4. Phase diagram of the D8/C4 mixtures obtained by polarizing microscopic observation on samples prepared with homeotropic boundary conditions.

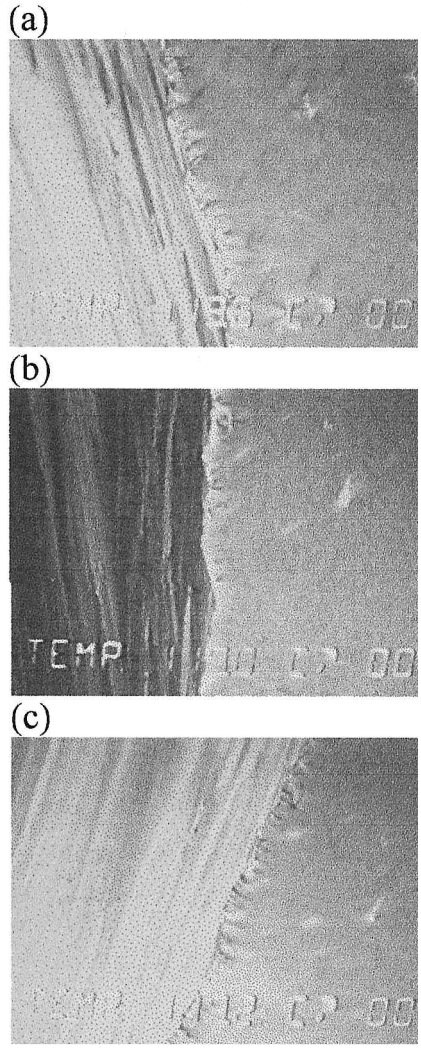


Figure 5. Verification of the TGBA* helical superstructure in the right part of the sample as compared to the ordinary SmA* phase (left). Turning the sample between crossed polarizers, only slight changes in birefringence are observed for TGBA*, while the SmA* phase can be brought into a dark position, when the director is oriented along one of the polarizer directions.

mixtures for samples with planar boundary conditions. An enhancement of the range of twist grain boundary phases with increasing concentration of the chiral dopant can be observed.

Preparation with homeotropic boundary conditions does not lead to the typical texture expected. A texture sequence obtained on cooling is shown in figure 3; the images resemble those one would expect to obtain for preparations without alignment layers ('natural textures'). Despite the homeotropic anchoring, the cholesteric phase still exhibits a Grandjean-like texture (*a*) and the TGBA* phase forms with a texture generally observed for preparations between untreated glass plates (*b*),

compare with [10]. The temperature region of the TGBA* phase stability is clearly smaller than for planar boundary conditions. Lowering the temperature, the transition to a SmA* phase is evidenced by the appearance of a fan-shaped texture (*c*). Further cooling gives no evidence for the existence of a TGBC* texture, but results in a SmA*–SmC* transition, indicated by the broken fan-shaped texture of figure 3 (*d*). The phase diagram of the D8/C4 mixtures for homeotropic boundary conditions is summarized in figure 4. From the texture studies, it can be deduced that the planar boundary conditions enhance the range of existence of the twist grain boundary phases observed.

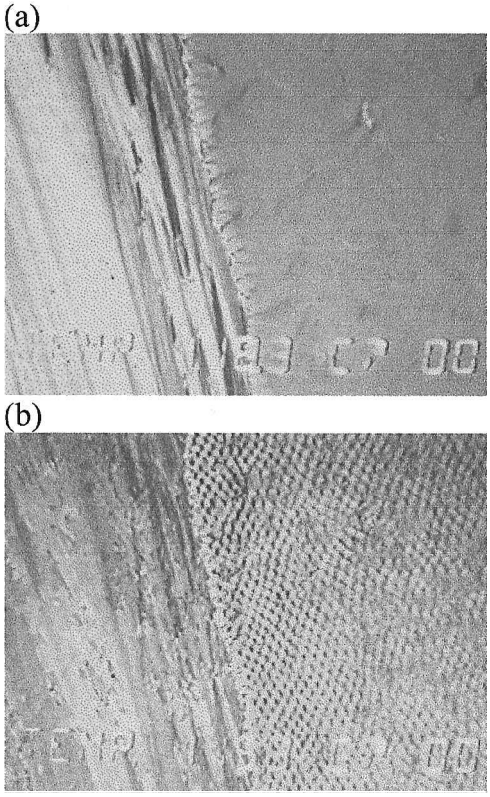


Figure 6. Demonstration for the 95%D8 + 5%C4 mixture of coexisting regions of: (*a*) SmA*/TGBA* with uniform planar texture (left) and helical Grandjean texture (right); (*b*) coexistence of SmC*/TGBC* with ferroelectric SmC* chevron domain texture (left) and square grid pattern (right). The image size is 290 μm × 220 μm.

To obtain evidence for the actual existence of the TGBA* phase, it has to be shown, that a helical superstructure is present. From the polarizing micrographs of figure 5, showing a sample with planar boundary conditions and coexisting regions of SmA* (left) and TGBA* (right), this can be deduced. While the SmA* phase can be brought into a dark position when the director points along one of the polarizer directions, the TGBA* phase exhibits a constant birefringence, when turning the sample between crossed polarizers. Optical activity on the other hand can be demonstrated by just turning the analyser. Thus the right part of figure 5 clearly exhibits a phase with a helical superstructure and helix axis parallel to the direction of light propagation.

As mentioned above, the occurrence of TGBA* and TGBC* phases under planar anchoring conditions is metastable within a certain range of temperatures. Under isothermal conditions SmA*/SmC* domains grow from the TGBA*/TGBC* phase. A region of phase coexistence is shown in figure 6 (*a*) for SmA*/TGBA* and figure 6 (*b*) for SmC*/TGBC*, as evidenced by the typical textures.

The nucleation of SmA*/SmC* domains and their growth process out from TGBA*/TGBC* is rather slow, in the region of several minutes. The process is clearly nucleation limited, as the nucleation time is about one to two orders of magnitude larger than the time of the actual growth process. Figure 7 shows an exemplary series of textures illustrating the growth of SmA* domains from the TGBA* phase of the 98%D8 + 2%C4

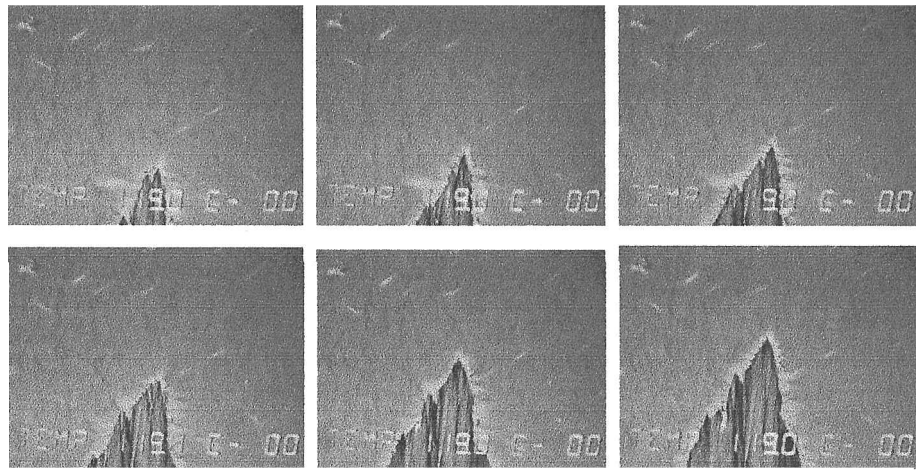

Figure 7. Sequence of texture photographs for the 95%D8 + 5%C4 mixture, taken at 3 s intervals, illustrating the growth of a SmA* domain into the TGBA* phase under isothermal conditions $T_{N^*/TGBA^*}$-$T$ = 3 K for planar boundary conditions.

mixture, three degrees below the N*–TGBA* transition, with images taken at 3 s intervals. From image analysis under isothermal conditions, a linear phase boundary displacement $d$ with time $t$ is observed, as shown for several temperatures within the TGBA* phase, figure 8 (*a*). From the respective plots, a phase boundary velocity $v$ can be obtained, which decreases with decreasing temperature, figure 8 (*b*). This behaviour may be attributed to the increasing viscosity as the temperature is lowered.

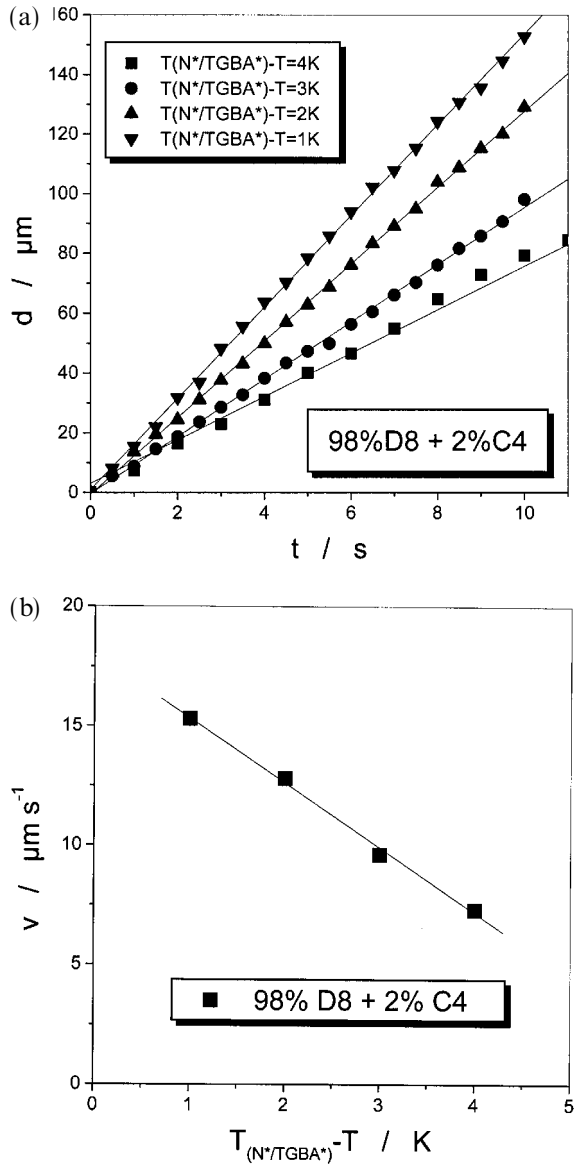


Figure 8. (*a*) SmA* phase boundary position $d$ as a function of time $t$ for several temperatures into the TGBA* phase under isothermal conditions for the 98%D8 + 2%C4 mixture; a linear growth process is observed. (*b*) The value determined for the phase boundary velocity $v$ decreases with decreasing temperature.

Again under isothermal conditions, three degrees below the cholesteric to TGBA* transition, a linear phase boundary displacement is observed with time for several concentrations of the chiral dopant, figure 9 (*a*). For the 80%D8 + 20%C4 mixture, no nucleation of SmA* regions from the TGBA* phase could be observed even after several hours. As shown in figure 9 (*b*), the respective phase boundary velocity strongly decreases

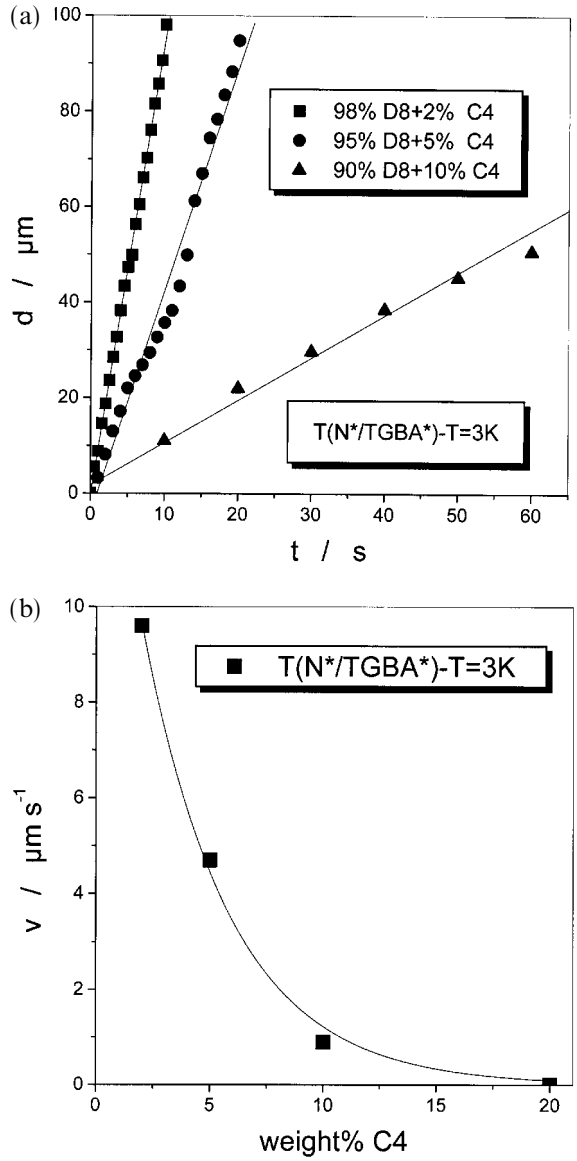


Figure 9. (*a*) SmA* phase boundary position $d$ growing into TGBA* as a function of time $t$ for several concentrations of the chiral dopant C4 under isothermal conditions $T_{N^*/TGBA^*}-T = 3$ K. For a sample with 20% of C4, no SmA* phase growth was observed. (*b*) The SmA* phase boundary velocity $v$ strongly decreases with increasing concentration of the chiral dopant C4, illustrating the stabilization of the TGBA* phase as the 'chirality' of the system is increased.

with increasing dopant concentration. Addition of a chiral dopant obviously enhances the tendency to preserve a twist grain boundary structure with respect to the conventional smectic phase. The phase boundary velocity of growing SmA* domains within the TGBA* phase should therefore be inversely proportional to a parameter describing the chirality of the system, such as the helical twisting power (HTP) of the chiral dopant. Qualitative evidence for this is given by the strongly reduced pitch of the cholesteric phase for mixtures with a large amount of C4 by about an order of magnitude as compared with pure D8.

## 4. Conclusions

Addition of a chiral dopant to a host material may induce twist grain boundary phases with a broad temperature range of existence. As compared with homeotropic anchoring, planar boundary conditions enhance the temperature range of TGB phases. Within the metastable TGBA*/TGBC* phase, the nulceation and growth of SmA*/SmC* regions is observed. This growth process proceeds linearly with time and exhibits a decreasing phase boundary velocity for decreasing temperature and increasing concentration of the chiral dopant.

I would like to thank A. Gembus for the preparation of the mixtures, D. Ganzke for providing the chiral dopant C4, and W. Haase for financial support. This work was supported by the Fonds der Chemischen Industrie.



## References

[1] Renn, S. R., and Lubensky, T. C., 1988, *Phys. Rev. A*, **38,** 2132.
[2] Goodby, J. W., Waugh, M. A., Stein, S. M., Chin, E., Pindak, R., and Patel, J. S., 1989, *Nature*, **337,** 449.
[3] Kitzerow, H.-S., 2000, in *Chirality in Liquid Crystals*, edited by Ch. Bahr and H.-S. Kitzerow (Berlin: Springer-Verlag), pp. 389–458.
[4] Kuczynski, W., and Stegemeyer, H., 1995, *Mol. Cryst. liq. Cryst.*, **260,** 377.
[5] Lavrentovich, O. D., Nastishin, Y. A., Kulishov, V. I., Narkevich, Y. S., and Tolochko, A. S., 1990, *Europhys. Lett.*, **13,** 313.
[6] Prasad, S. K., Raja, V. N., Nair, G. G., and Goodby, J. W., 1994, *Mol. Cryst. liq. Cryst.*, **250,** 239.
[7] Booth, C. J., Goodby, J. W., Hardy, J. P., and Toyne, K. J., 1994, *Liq. Cryst.*, **16,** 43.
[8] Sah, Y., 1997, *Mol. Cryst. liq. Cryst.*, **302,** 207.
[9] Kramarenko, N. L., Kulishov, V. I., Kutulya, L. A., Semenkova, G. P., Seminozhenko, V. P., and Shkolnikova, N. I., 1997, *Liq. Cryst.*, **22,** 535.
[10] Dierking, I., and Lagerwall, S. T., 1999, *Liq. Cryst.*, **26,** 83.
[11] Dierking, I., Giesselmann, F., and Zugenmaier, P., 1994, *Liq. Cryst.*, **17,** 17.
[12] Kuczynski, W., and Stegemeyer, H., 1997, *Proc. SPIE*, **3318,** 90.
[13] Kuczynski, W., in *Chiral Liquid Crystals*, edited by L. Komitov (Singapore: World Scientific) (to be published).
[14] Pratibha, R., Pramod, P. A., and Madhusudana, N. V., 1997, *Current Science*, **73,** 761.